Interactive Visualization of Terascale Data in the Browser: Fact or Fiction?

Will Usher* Valerio Pascucci
SCI Institute, University of Utah

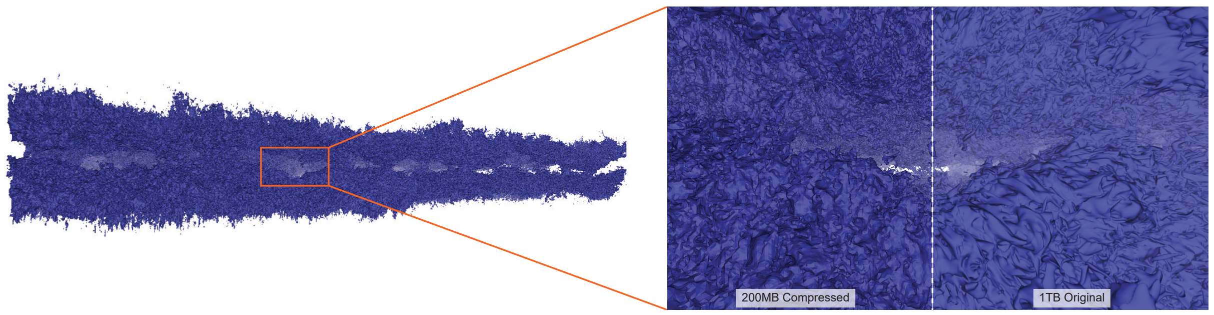

Figure 1: Interactive visualization of an isosurface of a ~1TB dataset entirely in the web browser. The full data is a float64 $10240\times7680\times1536$ grid computed by a DNS simulation [20, 21]. The isosurface is interactively computed and visualized entirely in the browser using our GPU isosurface computation algorithm for block-compressed data, after applying advanced precision and resolution trade-offs [14, 15, 24]. The surface consists of 137.5M triangles and is computed in 526ms on an RTX 2070 using WebGPU in Chrome and rendered at 30FPS at 1280×720. The original surface, shown in the right split image, consists of 4.3B triangles and was computed with VTK's Flying Edges filter [40] on a quad-socket Xeon server in 78s using 1.3TB of memory.

Abstract

Information visualization applications have become ubiquitous, in no small part thanks to the ease of wide distribution and deployment to users enabled by the web browser. Scientific visualization applications, relying on native code libraries and parallel processing, have been less suited to such widespread distribution, as browsers do not provide the required libraries or compute capabilities. In this paper, we revisit this gap in visualization technologies and explore how new web technologies, WebAssembly and WebGPU, can be used to deploy powerful visualization solutions for large-scale scientific data in the browser. In particular, we evaluate the programming effort required to bring scientific visualization applications to the browser through these technologies and assess their competitiveness against classic native solutions. As a main example, we present a new GPU-driven isosurface extraction method for block-compressed data sets, that is suitable for interactive isosurface computation on large volumes in resource-constrained environments, such as the browser. We conclude that web browsers are on the verge of becoming a competitive platform for even the most demanding scientific visualization tasks, such as interactive visualization of isosurfaces from a 1TB DNS simulation. We call on researchers and developers to consider investing in a community software stack to ease use of these upcoming browser features to bring accessible scientific visualization to the browser.

Index Terms: Web Applications; Parallel Isosurface Extraction

1 Introduction

Information visualization applications using D3 [7], Vega [37], Vega-Lite [36], and Tableau (formerly Polaris) [43] have become ubiqituous on the web, reaching millions of users to make data more accessible and understandable. The web browser platform is key to enabling this ubiquity, by providing a standardized, cross-platform environment through which applications can be deployed to users. Similarly, the browser eases the process by which users access an application and enhances security, removing the need to install and trust additional packages on their system. Although the browser has been widely used to deploy information visualization applications, this has not been the case for scientific visualization applications.

Scientific visualization applications often rely on native libraries (e.g., VTK [39]), fast floating point operations, large amounts of memory, and parallel processing or high-performance rendering on the GPU or CPU. Porting the required native libraries and rewriting the application to JavaScript is a significant undertaking, and does not address the computational demands of the application. As a result, the majority of web-based scientific visualization applications rely on a backend server to perform data processing and visualization (e.g., [12, 19, 33–35]), or to stream reduced representations of the data to reduce the demands placed on the browser (e.g., [16, 29, 41, 42]). Using a server gives the application access to significant computational resources, at the cost of latency for users and financial cost to the developer to run the servers. When considering a large-scale deployment, the cost of provisioning sufficient servers to meet demand is a real concern.

WebAssembly [4] and WebGPU [5] are new web technologies that can help address the issues faced when bringing scientific visualization applications to the browser. WebAssembly is a bytecode format to which native code can be compiled (e.g., through Emscripten [45]) and that can be executed at near-native speeds in the browser. WebGPU is a new low-level graphics API for the browser, similar in spirit to DirectX 12, Vulkan, and Metal, although it provides an easier-to-use API. WebGPU exposes advanced rendering and compute functionality to significantly expand the GPU capabilities available to browser applications compared to WebGL. WebGPU supports compute shaders and storage buffers, enabling arbitrary parallel computation on large data, and easing the implementation of such computation compared to prior efforts, which leveraged the WebGL rendering pipeline [22, 23].

In this paper, we perform an initial evaluation of how these new technologies can be leveraged to enable scientific visualization applications to run directly in the browser. We evaluate the performance of widely used native libraries for importing images and LIDAR data when compiled to WebAssembly, and the performance of Marching Cubes [27] as proxy for common floating point and memory

*will@sci.utah.edu

intensive scientific visualization algorithms. Finally, we propose a fully GPU-driven parallel isosurface extraction algorithm for interactive isosurfacing of block-compressed volume data on memory-constrained client devices to enable large-scale data visualization in the browser. Our isosurface extraction algorithm makes use of GPU decompression and a GPU-managed LRU cache to achieve interactive isosurface extraction with a small memory footprint. Our specific contributions are:

- An experimental assessment of WebAssembly and WebGPU as tools for building scalable scientific visualization applications, e.g., volume rendering, geospatial visualization, and isosurface computation, that execute entirely in the browser client without offloading computation to a server.
- A parallel isosurface extraction algorithm for resource-constrained platforms, such as the browser. The approach includes:
  - A GPU-driven parallel isosurface extraction algorithm capable of interactive isosurface computation for interactive data interrogation;
  - A GPU-driven memory management and caching strategy that allows working with compressed data on the GPU without CPU interaction;
  - Evaluation of our approach on up to 1B voxels and 1TB of volume data by applying state-of-the-art precision and resolution trade-offs.

2 Related Work

Even with the browser's prior limitations on graphics and compute capability, a number of works have explored methods for deploying scientific visualization in the browser, either through a client-server architecture or by leveraging the capabilities provided by WebGL. We review these works in Section 2.1. In Section 2.2 we review relevant work on parallel isosurface extraction algorithms.

2.1 Scientific Visualization in the Browser

A number of scientific visualization applications have used WebGL, a subset of OpenGL available in the browser, to perform rendering on the client [16, 29, 41, 42]. Mobeen and Feng [29] demonstrated a volume renderer in WebGL capable of high-quality interactive volume rendering of small data sets on mobile devices. Sherif et al. [42] presented BrainBrowser to allow interactive visualization of large-scale neuroimaging data sets fetched from a remote server. Recently, Li and Ma [22, 23] proposed an approach for parallel processing by leveraging the WebGL rendering pipeline to provide a subset of common data-parallel primitives. However, WebGL lacks support for compute shaders and storage buffers, making the implementation of general high-performance parallel primitives challenging.

To visualize large data sets, prior work has either streamed subsets of the data to clients for rendering [41, 42], or rendered it remotely on a server and streamed the resulting images back [12, 19, 33–35]. Remote rendering approaches allow the application access to arbitrary compute capabilities to process massive data sets, although these approaches can face challenges with latency and cost. When considering a large-scale deployment, e.g., data visualization on the home page of the New York Times, the cost of running sufficient servers to satisfy the large number of clients is a real concern. Fully client-side applications, our focus in this paper, move the computation and data to the clients. Users can then interact with the data locally, without added network latency.

In a recent survey of web-based visualization approaches, Mwalongo et al. [31] specifically mention latency and the lack of CUDA capabilities as key remaining challenges for visualization in the browser. By using WebGPU, applications that rely on GPU computing can now be run locally on the client, eliminating the cost of GPU virtual machines and latency. Access to powerful GPU capabilities can also ease the implementation of more advanced latency hiding techniques for hybrid client-server applications.

2.2 Parallel Isosurface Extraction

Isosurface extraction is a classic and widely used scientific visualization algorithm, and has received wide attention since the original Marching Cubes paper [27]. Livnat et al. [26] and Cignoni et al. [8] proposed to accelerate computation by skipping regions that are known to not contain the isosurface based on their range, using a range k-d tree or interval tree to accelerate the search. Approaches leveraging similar ideas for skipping regions, based on macrocell grids [32] and k-d trees [13, 44], have been proposed for implicit isosurface ray tracing, allowing the application to render the surface directly without storing additional vertex data.

A number of GPU parallel isosurface extraction algorithms have been proposed [2, 9, 11, 18, 25, 28, 38, 40]. GPU-parallel algorithms typically process each voxel in parallel in a thread, using prefix sums and stream compaction operations to output the vertices produced into a single buffer. Early work achieved the compaction step using HistoPyramids [11] and performed processing in the geometry shader; however, recent works [2, 25] in CUDA are able to leverage compute kernels for processing and Thrust [6] to provide fast prefix sum and stream compaction kernels. In contrast to our approach, existing algorithms assume the entire data set is able to fit in the memory of one GPU [2, 9, 11, 18, 25, 28, 38, 40], or be distributed among multiple GPUs in a cluster [28]

The block-based work decomposition approach proposed by Liu et al. [25] is most similar to our proposed algorithm. Liu et al. compute the value range of each block and use this information to filter out blocks that do not contain the isovalue. They then compute the number of vertices to be output by each block in parallel and perform a prefix sum to compute the output offsets for each block. A second pass computes and outputs the vertices for each voxel. Per voxel output offsets are computed using a prefix sum within the thread group processing a block, eliminating the need to store per voxel offsets or perform a global prefix sum. Within each block, vertices are computed using Flying Edges [40]. However, Liu et al. assume the entire data set is stored in a single 3D texture and only use the block decomposition to accelerate computation. In contrast, our approach does not store the full volume data. Instead, we decompress and cache only the blocks required to compute the surface using our GPU-driven LRU cache.

3 Revisiting the Browser as a Platform for Accessible Scientific Visualization

In this work, we are concerned with the capabilities available in the user's browser and the applications that can be developed by leveraging those capabilities. There are two recent technologies in the browser that can be used to develop powerful visualization applications: WebAssemby (Section 3.1) and WebGPU (Section 3.2).

3.1 WebAssembly

When considering bringing an existing scientific visualization application to the web, or deploying an entirely new one, a major concern is the lack of libraries widely used in native applications, e.g., for loading different data formats or performing computation. Previously, developers may have chosen to port the required libraries to JavaScript (e.g., VTK.js [3]), or recompile them to JavaScript using Emscripten [45]. Porting a substantial set of dependencies to JavaScript is clearly a major undertaking, and although Emscripten can compile C and C++ code to JavaScript, the performance of JavaScript is typically insufficient for computationally intensive tasks. Today, the above issues can be addressed by using Emscripten, or toolchains for other languages, to compile the required libraries to WebAssembly.

```
struct LASFile {
  LASreader *reader;
  std::vector<float> positions;
  LASFile(const char *fname);  // Reads file using LAStools
};
extern "C" LASFile* openLAS(const char *fname) {
  return new LASFile(fname);
}
extern "C" float* getPositions(LASFile *file){
  return file->positions.data();
}
extern "C" uint64_t getNumPoints(LASFile *file) {
  return file->positions.size() / 3;
}
```

```
// Setup call information for the exported C functions
var openLAS = Module.cwrap("openLAS", "number", ["string"]);
var getPositions =
    Module.cwrap("getPositions", "number", ["number"]);
var getNumPoints =
    Module.cwrap("getNumPoints", "number", ["number"]);
// Write file data into Emscripten's virtual filesystem
FS.writeFile("data.laz", new Uint8Array(fileData));
var lasFile = openLAS("data.laz");
// Create a view of the Wasm module's point data
var positions = new Float32Array(HEAPF32.buffer,
    getPositions(lasFile), getNumPoints(lasFile) * 3);
```

Listing 1: A subset of our C API (top) for the LASlib WebAssembly module and its use from JavaScript (bottom). The C API manages loading the data using LASlib and stores it in memory that can be shared with JavaScript. JS creates a view of the module's memory starting at the "pointer" returned by the API to access the data.

WebAssembly (Wasm) [4] is a standardized bytecode format for a virtual machine that can be run in the browser or natively. In contrast to Java Applets or Flash, WebAssembly is integrated natively into the browser, supporting tight integration with JavaScript and security through sandboxing, and is targetable by C and C++ through Emscripten. WebAssembly is shipping today in the major browsers, Chrome, Firefox, Safari, and Edge, ensuring wide availability on user systems. In a study of various compute benchmarks, Jangda et al. [17] found WebAssembly to be 1.5–3.4× slower than native code, depending on the task. These slowdowns can be partly attributed to enforcing WebAssembly's security guarantees, which require some additional checks to be performed.

3.1.1 Compiling Native Libraries to WebAssembly

The Emscripten compiler can be used as a drop in replacement C or C++ compiler and can compile most portable code to WebAssembly[1]. The main challenge when compiling a library to WebAssembly is the number of dependencies required by the library, as each one must also be compiled to WebAssembly. Large libraries such as VTK [39], whose dependencies may themselves have a number of dependencies, can produce a large graph of libraries that must all be compiled to WebAssembly to link against.

To provide a convenient API for calling into C++ libraries from JavaScript and working with C++ objects, library authors can use the binding generation tools provided by Emscripten: WebIDL Binder (similar to SWIG) or Embind (similar to Boost.Python). For smaller libraries or minimal bindings, it is also possible to export a C API and call it directly from JavaScript.

We discuss two applications that use native libraries compiled to WebAssembly. The Neuron Visualization example (Section 3.3.1), which uses the C libtiff library to load TIFF image stacks, and the LIDAR visualization example, which uses the C++ LASlib [1] library to load las and laz LIDAR data files. The libtiff library depends on zlib and libjpeg, and thus we had to first compile these libraries to Wasm and link them with libtiff to produce the library. For LASlib, we wrote a minimal C API (Listing 1) to discuss the lower level details of calling between JavaScript and C or C++ Wasm modules. Our libtiff[2] and LASlib[3] WebAssembly modules are available on Github.

[1]https://emscripten.org/docs/porting/guidelines/index.html

3.1.2 Sharing Memory Between JavaScript and WebAssembly Modules

The heap space of a WebAssembly module is stored within a JavaScript ArrayBuffer object that can be grown to meet dynamic allocation needs of the module (i.e., `malloc` and `new`). Pointers in the module are simply offsets into this ArrayBuffer. Thus, the module can directly share memory with the JavaScript host code by returning a pointer that can be used to create a view of the module's heap starting at the returned index. We use this approach to share the point cloud data loaded by our LASlib module with JavaScript without copying (Listing 1).

However, it is not possible for WebAssembly modules to directly see JavaScript memory. To pass an array of data from JavaScript to a module, space must be allocated from the module's heap to copy the array into. The index to which the array was written in the heap is then passed to the module as a pointer. To minimize the number of such copies that must be made to pass arrays to the module, it is best to have the module store large arrays in its heap and have JavaScript create an array view of the heap.

3.2 WebGPU

WebGPU [5] is a modern graphics API for the web, in development by the major browser vendors and available for testing in the preview builds of Chrome, Firefox, and Safari. WebGPU fills a role similar to Vulkan, DirectX 12, and Metal, providing a low-level API with more explicit control to the user and fixed inputs to the driver, allowing for improved performance compared to WebGL. Moreover, WebGPU exposes additional GPU functionality that is key to implementing general parallel compute algorithms, providing access to compute shaders, storage buffers, and storage textures.

The concepts used in WebGPU should be familiar to users of Vulkan, DirectX 12, and Metal, though WebGPU is not as "low level" as the native APIs, striking a good balance between usability and performance. In WebGPU, rendering or compute passes are recorded using a command encoder to buffer up and submit work to the GPU. When recording a pass, a rendering or compute pipeline can be bound. The pipeline specifies the shaders to run, the layout of buffer inputs to the shaders, and, for rendering pipelines, the layout of vertex attributes and output render targets. Groups of buffers and textures matching the specified layouts can be bound to pass data to the shaders. The fixed layout of the pipeline allows the GPU to optimize its execution while the data being processed can still be changed as needed. This fixed layout is in contrast to WebGL and OpenGL, where the entire rendering or compute state cannot be provided to the driver in advance, limiting the optimizations that can be performed.

3.3 Example Applications and Performance vs. Native Execution

In this section, we evaluate a set of example applications for common visualization tasks that make use of WebAssembly and WebGPU. The applications cover a range of common operations performed in visualization: loading TIFF image stacks of microscopy volumes (Section 3.3.1), interactive visualization of LIDAR data (Section 3.3.2), naive serial and data-parallel isosurface extraction (Section 3.3.3), and volume decompression (Section 3.3.4). For each example we provide a performance comparison against native code on the same task, to assess the capabilities of WebAssembly and WebGPU for scientific visualization applications.

[2]https://github.com/Twinklebear/tiff.js
[3]https://github.com/Twinklebear/LAStools.js

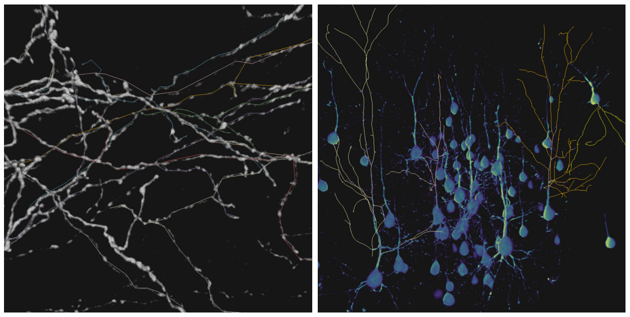
Figure 2: Images of the neuron visualization application, used by neuronatomists to judge the quality of neuron reconstructions (rendered as lines) in the browser.

Dataset	Native	Firefox 78	Chrome 83
Layer 1 Axons (44MB, 76 files)	0.87s	1.8s	2.6s
Cell Bodies (263Mb, 314 files)	4.1s	8.6s	16s

Table 1: Load times for the connectomics data sets using the native build of libtiff and the WebAssembly module in Firefox and Chrome.

3.3.1 Neuron Visualization

The first example is a web application for visualization of connectomics data (Figure 2). The application uses libtiff compiled to WebAssembly to import TIFF stacks which are volume rendered using WebGL2. TIFF files are loaded by writing the file data into Emscripten's virtual in memory filesystem, after which the file name can be passed to `TIFFOpen` and read through Emscripten's implementation of the POSIX file API. The application can also import SWC files to display neuron reconstructions with the volume data. This tool was written to facilitate collaboration on another project, allowing visualization researchers to easily collect feedback from neuroanatomists on reconstruction quality. The neuroanatomist is able to simply open the web page, upload the data and traces, and interactively compare multiple reconstructions. We chose WebGL2 for the rendering component of this tool to ease deployment, as WebGPU is not yet available outside preview browser builds.

Performance We compare time to load two connectomics data sets using our WebAssembly build of libtiff and the native version in Table 1. The benchmarks are run on a Surface Pro 7 laptop with an i5-1035G4 CPU and 8GB of RAM. We find that, similar to the results reported by Jangda et al. [17], WebAssembly is 2-4× slower than native code. The browser's implementation of the WebAssembly engine is an important factor, with Firefox outperforming Chrome by 2×.

3.3.2 LIDAR Visualization

Our second application example is LIDAR visualization, a common task in geospatial applications. To enable loading LIDAR data directly in the browser, we compiled the widely used library LAStools [1] to WebAssembly. LAStools has no external dependencies, making it easy to compile to Wasm; however, it is a C++ library and thus requires a C API to be written or generated to be called from JavaScript. We wrote a minimal C API over the library that supports loading files and retrieving the contained points and colors to provide an illustrative example of the process (see Listing 1 and Github[3]). Laz files uploaded by the user are written into Emscripten's virtual filesystem to allow the library to open them. The loaded points are then rendered as billboarded quads using WebGPU (Figure 3) to display varying size round or square points.

Performance We compare the time to load various compressed LIDAR data files in laz format, from 9M to 40M points, using the native and WebAssembly versions of LAStools in Table 2. For these benchmarks, we use Chrome Canary and Firefox Nightly, as they are required for WebGPU support. The benchmarks are performed on a Surface Pro 7. As before, we find that Firefox's WebAssembly engine is 2-3× slower than native code, with Chrome's engine an additional 2-3.5× slower than Firefox. Although performance trails native code overall, the loading times achieved for the data sets are likely acceptable in an application.

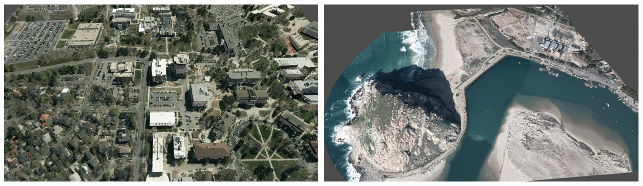
(a) Utah 9M, points (b) Morro Bay, 40M points

Figure 3: Images from our WebGPU LIDAR renderer. At 1280×720 the images render at (a) 100 FPS and (b) 35FPS on an RTX 2070, and (a) 14FPS and (b) 3.5FPS on a Surface Pro 7.

Dataset	Native	Firefox 80	Chrome 86
Utah 9M	3.8s	9.2s	29s
Morro Bay 20M	7.8s	20s	68s
Utah 30M	13s	30s	100s
Morro Bay 40M	16s	41s	133s

Table 2: Load times for the laz files using the native build of LASlib and the WebAssembly module in Firefox and Chrome.

In Figure 3 we report the rendering performance achieved by our LIDAR renderer on the smallest and largest data sets tested, on both a Surface Pro 7 and a desktop with an RTX 2070 GPU. We find that our basic renderer, which does not employ level of detail or filtering to accelerate rendering, is still able to provide interactive rendering of the largest data set even on the integrated GPU of the Surface Pro.

3.3.3 Marching Cubes

While our prior examples have focused on I/O and memory intensive tasks, namely, loading compressed and complex data formats, another key concern is the performance of compute intensive tasks. We use Marching Cubes [27] as a representative proxy for the compute demands of common analysis tasks performed in scientific visualization applications. We evaluate the performance of serial implementations in C++, JavaScript, and WebAssembly, and data-parallel variants in Vulkan and WebGPU. Our data-parallel variants are similar to standard approaches using CUDA [2, 10]: a compute shader run over all voxels marks those containing the surface, the active voxel IDs are then compacted using a GPU prefix sum and stream compaction. For each active voxel, a compute shader determines the number of output vertices and writes the result to a global buffer. The offsets for each voxel and total number of vertices are computed using a GPU prefix sum. A second pass over the active voxels computes and outputs the vertices to produce a triangle soup.

Performance We compare our serial implementations on the Surface Pro 7 on four small data sets, ranging in size from 64^3 to 256^3. As before, we use Chrome Canary and Firefox Nightly. We compute 100 random isovalues using each variant and report the average time to compute the surface. The 100 random isovalues are sampled over a range covering surfaces typically of interest to users, excluding noise and values so high as to produce few output triangles.

For our serial implementations (Figure 4), we find that our WebAssembly version run in Firefox is on average only 1.5× slower than native code. Firefox's JavaScript engine is on average 4.4× slower than native code, with the performance gap between JavaScript and WebAssembly increasing with data set size. Chrome's WebAssembly performance is on par with its JavaScript performance, averaging 3.2× and 3.6× slower than native code, respectively.

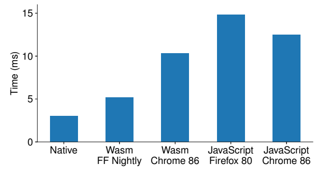

(a) Fuel (64^3)

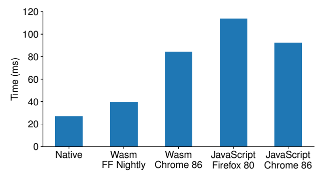

(b) Hydrogen Atom (128^3)

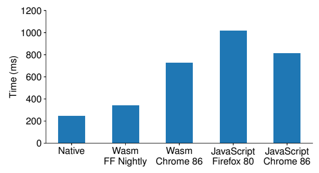

(c) Bonsai (256^3)

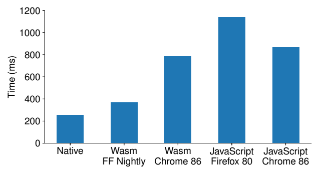

(d) Skull (256^3)

Figure 4: Performance of our serial C++, JavaScript, and WebAssembly versions of Marching Cubes on 100 random isovalues.

Dataset	Vulkan	WebGPU
Fuel 64^3	25ms	26ms
Hydr. 128^3	58ms	86ms
Bonsai 256^3	228ms	261ms
Skull 256^3	279ms	282ms
Plasma 512^3	1357ms	$*$

(a) Surface Pro 7

Dataset	Vulkan	WebGPU
Fuel 64^3	2ms	18ms
Hydr. 128^3	8ms	18ms
Bonsai 256^3	49ms	49ms
Skull 256^3	70ms	50ms
Plasma 512^3	322ms	329ms

(b) RTX 2070

Table 3: Performance of our naive data-parallel Marching Cubes implementation on 100 random isovalues. We find that WebGPU performance is typically on par with native Vulkan code. $*$ failed on the Surface Pro.

We compare our data-parallel versions on the Surface Pro 7 and a desktop with an RTX 2070 (Table 3), and test on an additional 512^3 data set. In each benchmark, we discard the first computation as we have found WebGPU to have a high first launch overhead. On the Surface Pro, we find moderate improvement over the fastest serial implementation in the browser on larger data sets, although both the Vulkan and WebGPU variants achieve performance just on par with the serial C++ version. When compared to the fastest WebAssembly version, the Bonsai and Skull see performance improvements of $\sim 1.3\times$. On the RTX 2070, we find significant performance improvements over the serial implementations, achieving a $7\times$ improvement on the 256^3 data sets over WebAssembly in Firefox, and a $5\times$ improvement over our serial native implementation.

The most exciting takeaway from our evaluation is that the performance of WebGPU is typically on par with native Vulkan code, indicating that little performance is lost when moving GPU compute kernels to the browser. On smaller data sets, we find WebGPU to be slower, where overhead in the WebGPU mapping layer to the underlying native graphics API may impact performance. This overhead is hidden on larger data sets, where the computation dominates the total execution time.

3.3.4 ZFP Decompression

When visualizing large-scale data on a remote client (e.g., the 1TB volume shown in Figure 1), transferring the entire data set to the client can be impractical or impossible. To reduce bandwidth and memory requirements, we can transfer a compressed version of the data, that the client can decompress as needed. ZFP [24] provides fast and high-quality compression of floating point scientific data, and is especially suited to large volumetric data. ZFP compresses volumetric data in 4^3 blocks, using fixed or variable bitrate compression. ZFP's fixed rate compression mode can be quickly compressed and decompressed in parallel on the GPU, and a CUDA implementation is provided with the library. To enable fast decompression of large data in the browser, we ported ZFP's CUDA decompressor to WebGPU, and to Vulkan to provide a native comparison point.

Dataset	CPU (Serial)	Vulkan	WebGPU
Skull 256^3	329MB/s	756MB/s	697MB/s
Plasma 512^3	349MB/s	898MB/s	777MB/s

(a) Surface Pro 7

Dataset	CUDA	Vulkan	WebGPU
Skull 256^3	67.1GB/s	14.8GB/s	7.6GB/s
Plasma 512^3	67.8GB/s	19.4GB/s	11.8GB/s
Miranda 1024^3	113GB/s	19.6GB/s	13.7GB/s

(b) RTX 2070

Table 4: ZFP decompression performance of our WebGPU implementation compared to a native Vulkan version and ZFP's original CUDA and serial decompressor. We find that neither our Vulkan nor WebGPU implementation is on par with the original CUDA implementation, though are still capable of fast parallel decompression.

Performance We compare our WebGPU and Vulkan ports of ZFP's CUDA decompressor on three data sets, on both a Surface Pro 7 and RTX 2070 (Table 4). For each data set, we compress it at three different bitrates, two, four, and eight, and report the average decompression performance of 10 runs. We use ZFP prerelease version 0.5.5-rc1 built from Github. As CUDA is not available on the Surface, and parallel decompression with OpenMP is not supported in ZFP, we compare our WebGPU and Vulkan variants to ZFP's serial decompressor on the CPU. The decompressed output of the largest data set, Miranda (4GB), does not fit in the Surface's 3.8GB VRAM, and thus we evaluate only the smaller data sets.

Although we achieve slightly over $2\times$ faster decompression on the Surface compared to the serial CPU decompressor, both our WebGPU and Vulkan versions are slower than the CUDA decompressor, by up to $8\times$ and $6\times$ on the Miranda. We also find the WebGPU implementation to trail the Vulkan version slightly, as observed previously. Although our implementations have room for improvement compared to ZFP's CUDA decompressor, the performance improvements over serial decompression are substantial.

4 Parallel Isosurface Extraction from Block-Compressed Data using WebGPU

Based on the performance results observed on the example applications, we conclude that the browser can provide a capable environment for scientific visualization tasks. However, working with large data sets in the browser using WebGPU is challenging due to limitations on network transfer bandwidth and GPU memory, requiring a combination of adaptive precision and resolution compression (e.g., [14, 15, 24]).

To enable interactive isosurface computation on large-scale data in the browser, we build on the following observations. First, the isosurfaces of interest to users typically occupy a sparse subset of the volume, which likely does fit in memory. Users are also likely to explore nearby isosurfaces, touching the same regions of the volume repeatedly. Third, ZFP's fixed-rate compression mode allows specific 4^3 blocks to be decompressed, without decompressing the entire data set. Finally, we find WebGPU performance to be on par with native, and thus pushing as much computation as possible to the GPU will be beneficial for processing large data sets.

These observations motivate the design of our GPU parallel algorithm for isosurface computation on block-compressed data (Figure 5 and on GitHub[4]). We begin by uploading the ZFP fixed-rate compressed data to the GPU, allowing us to decompress blocks as needed without additional interaction with the CPU. To compute the isosurface, we first find the blocks containing the data required to compute it (Section 4.1). We then determine which of these blocks

[4]https://github.com/Twinklebear/webgpu-bcmc

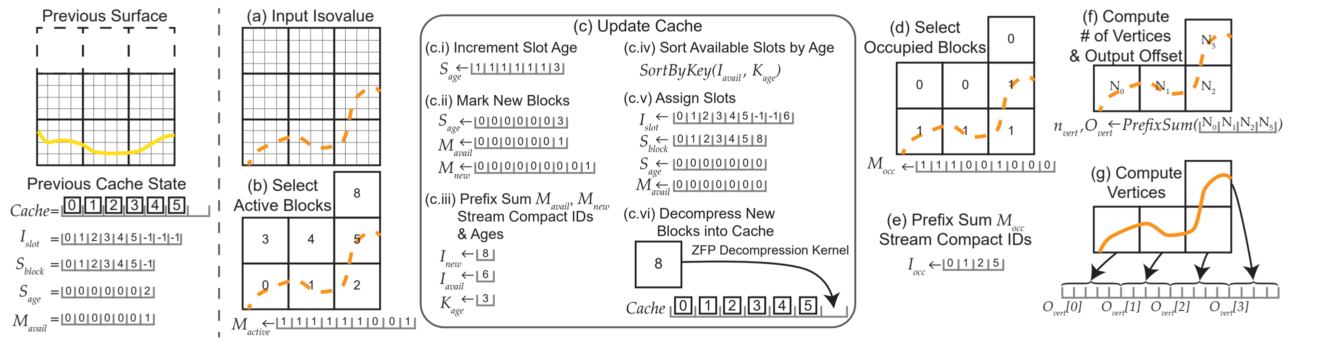
Previous Surface
Previous Cache State
(a) Input Isovalue
(b) Select Active Blocks
(c) Update Cache
(c.i) Increment Slot Age
(c.ii) Mark New Blocks
(c.iii) Prefix Sum M_{avail}, M_{new} Stream Compact IDs & Ages
(c.iv) Sort Available Slots by Age
$SortByKey(I_{avail}, K_{age})$
(c.v) Assign Slots
(c.vi) Decompress New Blocks into Cache
ZFP Decompression Kernel
(d) Select Occupied Blocks
(e) Prefix Sum M_{occ} Stream Compact IDs
(f) Compute # of Vertices & Output Offset
$n_{vert}, O_{vert} \leftarrow PrefixSum([N_0|N_1|N_2|N_5])$
(g) Compute Vertices
$O_{vert}[0]$ $O_{vert}[1]$ $O_{vert}[2]$ $O_{vert}[3]$

Figure 5: An illustration of our parallel isosurface algorithm in 2D. Starting from an existing cache used to compute a previous surface (or an empty one) we wish to compute the surface at the new isovalue in (a). (b) We find the blocks that contain the isovalue or are needed to provide neighbor data for blocks containing it. (c) We determine which of these blocks are already in the cache and those that must be decompressed and added to it (also see Algorithm 1). (d) The active blocks are filtered down to just those that will output vertices, (e) after which we compute the number of vertices that will be output by each block and (f) output them to a single vertex buffer.

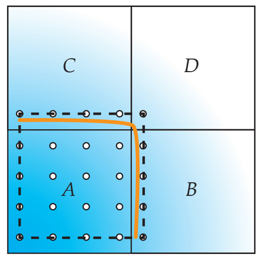

Figure 6: The dual grid of block A (dashed) overlaps its neighbors B, C, D, who must also be decompressed to provide the data required to compute the surface (orange).

are in the cache or must be added to it (Section 4.2). Each new block is assigned a slot in the cache and decompressed into it (Section 4.2.1). Active blocks are processed by loading them and the required neighbor voxels into shared memory (Section 4.3). For each active block, we compute the number of vertices output by its voxels (Section 4.4). Finally, for each block that will output vertices, we compute the vertices to output a triangle soup (Section 4.5).

4.1 Selecting Active Blocks

As done by Liu et al. [25], we precompute and store the value range of each block when loading the data. To find active blocks, we run a compute shader over the blocks that marks a block as active if its range contains the isovalue (Figure 5b). However, in contrast to Liu et al., we do not have access to the full volume in a 3D texture. Thus, marking only the blocks containing the isovalue as active is not sufficient, since the data required for their dual grid cells sharing vertices with neighboring blocks would be missing (Figure 6). To ensure the neighbor data is available, we mark a block as active if its range or the union of its range and any of its neighbors' ranges contain the isovalue. The output of our kernel is the active mask list M_{active}. The list of active block IDs, I_{active}, is computed using a GPU prefix sum and specialized stream compaction, "StreamCompactIDs". The specialized compaction writes the element's index in the active mask list at the output offset (computed in the prefix sum) instead of the element's value, compacting the IDs of the active elements.

4.2 GPU-driven LRU Block Cache

Given M_{active} and I_{active}, we determine which active blocks are already in the cache and which must be decompressed and added to it. This task is performed using an entirely GPU-driven LRU cache, allowing us to avoid reading back M_{active} or I_{active} to the host and to minimize the amount of serial computation.

The cache is comprised of a growable number of "slots", within which a decompressed block can be stored. The initial number of slots is set by the user, e.g., enough to store 10% of the blocks in the volume. We use two arrays to track the status of each slot: S_{age},

```
1: function UPDATECACHE($M_{active}$)
2:     $IncrementSlotAge(S_{age})$
3:     $M_{new}, M_{avail} \leftarrow MarkNewBlocks(M_{active}, S_{age}, I_{slot})$
4:     $n_{new}, O_{new} \leftarrow PrefixSum(M_{new})$            ▷ Exit if $n_{new} = 0$
5:     $n_{avail}, O_{avail} \leftarrow PrefixSum(M_{avail})$ ▷ Grow if $n_{new} > n_{avail}$
6:     $I_{new} \leftarrow StreamCompactIDs(M_{new}, O_{new})$
7:     $I_{avail} \leftarrow StreamCompactIDs(M_{avail}, O_{avail})$
8:     $K_{age} \leftarrow StreamCompact(M_{avail}, O_{avail}, S_{age})$
9:     $SortByKey(I_{avail}, K_{age})$            ▷ Sort available slots by age
10:    $AssignSlots(I_{new}, I_{avail}, S_{age}, S_{block}, I_{slot})$
11:    $DecompressBlocks(I_{new}, I_{slot})$
```

Algorithm 1: Our GPU-driven cache update algorithm. Each function call corresponds to a compute shader dispatch or data-parallel primitive (prefix sum, stream compact, sort) run on the GPU.

which stores the age of the item in the slot, and S_{block}, which stores the ID of the block in the slot or -1 if the slot is empty. An additional array, I_{slot}, stores the ID of the slot occupied by each block, or -1 if the block is not cached. Finally, we maintain a buffer storing the actual data for each slot, containing the decompressed 4^3 block.

Our GPU parallel cache update proceeds as shown in Algorithm 1 (also see Figure 5c). First, we increment each slot's age in parallel using a compute shader. We then compute a list M_{new} that marks, for each block, if it must be newly decompressed and added to the cache; and update the list M_{avail} that marks, for each slot, if it is available. To compute M_{new} and M_{avail}, we run a compute shader for each block b that checks if it is active (i.e., $M_{active}[b] = 1$). If the block is active and cached (i.e., $I_{slot}[b] \neq -1$), the thread resets the age of its slot, marks the slot unavailable in M_{avail}, and marks the block as not new in M_{new}. If the block is active and not cached, it is marked as new. If a block is cached and not active its slot is marked as available, making it a candidate for eviction. We then perform a GPU prefix sum on M_{new} and M_{avail} to compute the number of new blocks and the number of available slots. If there are no new blocks, we can terminate the update, if fewer slots are available than are needed, the cache is grown. New slots added when growing the cache are marked available and assigned a high age.

We then use "StreamCompactIDs" to compute the list of new block IDs, I_{new}, and available slots, I_{avail}. The active list and output offsets come from M_{new}, O_{new} and M_{avail}, O_{avail}, respectively. The available slot ages, K_{age}, are computed with a standard stream compaction using the output offsets O_{avail}. I_{avail} is then sorted in descending order by age using a GPU sort by key, where K_{age} contains the keys. Finally, we assign each new block a slot s from I_{avail} using a compute shader run for each new block. If a block p was previously stored in the slot (i.e., $S_{block}[s] \neq -1$), it is evicted by setting $I_{slot}[p] = -1$. The new block is then set as the item in the slot, the slot assigned to the block in I_{slot}, the slot marked unavailable, and the slot age reset to 0.

4.2.1 Decompression of Blocks into Cache Slots

We use our WebGPU port of ZFP's CUDA decompressor from Section 3.3.4, modified to decompress just the blocks specified in I_{new}. Each new block b is decompressed by a thread on the GPU in a compute shader. The thread writes the 4^3 decompressed block as a row-major array into the cache slot assigned to the block ($I_{slot}[b]$). This approach has the added benefit of eliminating the scattered writes required when outputting the entire volume, improving the write access patterns of each decompression thread.

4.3 Loading Blocks and Neighbor Voxels into Shared Memory

To compute the vertices of each block, we need the data for it and its neighbors in the $+x/y/z$ direction, with which the block's dual grid shares vertices (Figure 6). As we do not store the full volume, accessing the neighbor voxels cannot be done with a 3D texture lookup as done by Liu et al. [25]. Instead, we load the data for the block's dual grid into shared memory to enable fast access to the data by the thread group processing the block. This step is performed by both the vertex output location computation (Section 4.4) and the final vertex computation (Section 4.5). In both steps, we assume the block has neighbors along all axes, i.e., a 4^3 dual grid, and we run a thread group per block with 64 threads, one thread per dual cell.

First, the group loads the 64 voxels of the 4^3 block into shared memory, with each thread loading a voxel. If the block has neighbors to its positive side we increase the block dimensions along the corresponding axis by one. However, we cannot assume the required face, edge, and corner neighbors exist, as only the active blocks are guaranteed to be decompressed and in the cache. For example, a block that is marked active because it is needed by a neighbor may not have any of its $+x/y/z$ neighbors active, and would thus attempt to load invalid data. After tentatively increasing the block's dimensions based on its location in the grid, we test if the required neighbors are active in M_{active}. If the required face, edge, or corner neighbor in some direction is not active, we reset the block's size along that direction to 4.

We then load the required neighbor data from the neighbor blocks. The threads responsible for the block's face, edge, and corner voxels are also responsible for loading the neighboring face, edge, and corner voxels, respectively. Finally, we synchronize the thread group using a barrier to wait until the data is loaded.

4.4 Computing Vertex Output Locations

Our next step is to determine the output offsets for each block's vertices and the total number of vertices to be output. Before doing so, we run a compute shader over the active blocks to determine the subset that will output vertices (Figure 5d). Each thread group loads a block into shared memory as described in Section 4.3. Each thread then checks if its dual cell will output a triangle and writes this result to shared memory. If the block will output a triangle, thread 0 marks the block as occupied in M_{occ}; otherwise, it is marked as empty. The list of occupied block IDs, I_{occ}, are found through a GPU prefix sum over M_{occ} and "StreamCompactIDs" (Figure 5e). It is not sufficient to mark unoccupied each block that was marked active as a result of the union of it and one of its neighbors' ranges, as the block's dual cells shared with the neighbor may output vertices that the block is responsible for computing (Figure 6). However, it may be possible to determine this by checking which side the neighbor was on.

We then compute the output offsets for each occupied block's vertices (Figure 5f). After loading the block and neighbor data into shared memory, we proceed as described by Liu et al. [25] to compute the vertex output offsets. Each thread computes the number of vertices that will be output by its dual cell and writes this value to shared memory. The thread group then performs a sum reduction to compute the total number of vertices that will be output by the block, which thread 0 writes to global memory. The per block output offsets and total output size are computed by a GPU prefix sum over the per block vertex counts. As suggested by Liu et al., we do not perform a global prefix sum or store the per voxel prefix sums computed within each block.

4.5 Vertex Computation

Each thread group loads an occupied block into shared memory and computes the number of vertices that will be output by each voxel as before, writing the result to shared memory. The thread group then performs a parallel prefix sum over this shared memory to compute the per voxel output locations relative to the block's global offset. Each thread then computes the vertices for its dual cell and writes them to the global vertex buffer (Figure 5g). Outputting an indexed triangle mesh using Flying Edges [40] within each block, as proposed by Liu et al. [25], is also possible.

To reduce the memory required to store the vertex buffer, we adopt a compressed vertex format. Vertices are stored relative to the block origin and quantized to 10 bits per coordinate. For each vertex, we store the three 10 bit coordinates packed into a uint32, along with the block ID as a second uint32, for a total of 8 bytes per vertex. Blocks are indexed in row-major order, providing a straightforward mapping from ID to 3D position in the volume. When rendering, we compute the block position from its ID and use it to offset the dequantized vertex.

4.6 Performance Evaluation

We evaluate our approach on nine data sets, varying in size and isosurface topology (Table 5). As ZFP only supports floating point data, we convert the non-float data sets to 32 bit floating point before compressing them. ZFP is able to compress the data sets to far less than 8 or 16 bits per voxel, and bitrates as low as 2 have been demonstrated to have low impact on quality [24]. Our benchmarks are run on a Surface Pro 7 with an integrated GPU with 3.8GB of VRAM and a desktop with an RTX 2070 with 8GB of VRAM.

The isosurfaces used in our evaluation can be classified into "nested" and "turbulent sheet" topologies, and have different cache behaviors. Isosurfaces with nested topologies are typical in MRI and CT scans (Skull, Foot, Backpack, Stag Beetle, Kingsnake, and Chameleon), although they do occur in simulations as well (Plasma). In the nested topology isosurfaces, surfaces at lower values enclose those at higher values. Such isosurfaces can be extremely cache friendly, as after computing a surface at a lower value, a large number of the blocks will be reused for neighboring surfaces, and even distant enclosed ones.

Isosurfaces with turbulent sheet topologies are typically found in simulations where the surface represents a moving interface, e.g., fluids mixing or turbulent flows (Miranda and DNS). In a turbulent sheet topology isosurface, surfaces move along one or more axes of the domain with the isovalue, and do not enclose each other. Moreover, the turbulent nature of the surface results in a large number of blocks being occupied and output triangles. Isosurfaces with turbulent sheet topology tend to be less cache friendly for random isovalues, as different surfaces occupy different and distant regions of the domain, with relatively few shared blocks; however, neighboring isovalues do share blocks as the surface does not make large jumps in the domain.

4.6.1 Isosurface Extraction

We perform three benchmarks on each data set, covering different levels of cache friendliness and user interaction modes when exploring a volume. The first benchmark computes 100 random isovalues, as in Section 3.3.3, representing a cache-unfriendly exploratory use case. The other two benchmarks sweep the isosurface up or down the data set's value range, as may be done when comparing neighboring values in the data, and are relatively cache friendly.

Image	Original	Adaptive Precision & Resolution	Isovalue	% Active	Cache Size	% Occupied	Triangles	Vertex Data
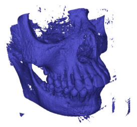	256^3 67.1MB	4.1MB $\approx \frac{1}{16}$ data size	39	38.9%	26MB	19.8%	2.1M	51MB
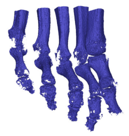	256^3 67.1MB	4.1MB $\approx \frac{1}{16}$ data size	117	11.7%	7.8MB	5.9%	743K	18MB
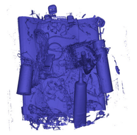	512×512×373 391MB	49.3MB $\approx \frac{1}{8}$ data size	409	22.6%	89MB	9.9%	6.2M	148MB
	512^3 537MB	67MB $\approx \frac{1}{8}$ data size	1.19	15%	81MB	9%	9.5M	229MB
	832×832×494 1.37GB	86MB $\approx \frac{1}{16}$ data size	868	5%	70MB	3%	6.7M	160MB
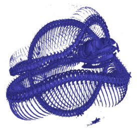	1024×1024×795 3.33GB	209MB $\approx \frac{1}{16}$ data size	111	5%	167MB	2%	10.2M	245MB
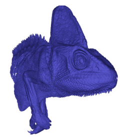	1024×1024×1080 4.53GB	283MB $\approx \frac{1}{16}$ data size	21290	4.5%	227MB	1.9%	11.2M	270MB
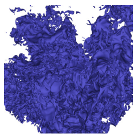	1024^3 4.3GB	537MB $\approx \frac{1}{8}$ data size	1.39	26%	1.1GB	12%	67M	1.6GB
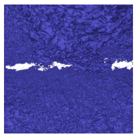	10240×7680×1536 966GB	199MB $\approx \frac{1}{4854}$ data size	0.936	43%	1.4GB	24%	135M	3.3GB

Table 5: Example isosurfaces on the data sets used in our benchmarks. Isosurfaces are typically sparse, requiring little data to be decompressed and cached to compute each surface, and even fewer blocks to be processed to compute the surface geometry.

	Random			Sweep Up			Sweep Down		
Dataset	Hit Rate	RTX 2070	Surface Pro 7	Hit Rate	RTX 2070	Surface Pro 7	Hit Rate	RTX 2070	Surface Pro 7
Skull	98.4%	57.7ms	99.8ms	100%	54.4ms	85.1ms	94.8%	93.1ms	161.5ms
Foot	98.9%	57.1ms	107.9ms	100%	58.4ms	99.2ms	97.4%	90.1ms	164.4ms
Backpack	99.4%	68.1ms	251.0ms	100%	99.1ms	216.3ms	96.8%	109.7ms	349.3ms
Plasma	96.4%	107.2ms	318.6ms	99.8%	94.3ms	265.3ms	98.5%	126.1ms	431.8ms
Stag Beetle	98.2%	123.1ms	322.1ms	99.6%	125.1ms	337.8ms	92.0%	151.2ms	464.5ms
Kingsnake	99.2%	212.6ms	926.5ms	100%	185.3ms	811.1ms	97.0%	284.5ms	1306ms
Chameleon	90.9%	371.6ms	1342ms	98.9%	348.7ms	1470ms	96.6%	337.1ms	1482ms
Miranda	46.8%	2218ms	(oom)	95.7%	550.5ms	(oom)	95.2%	549.6ms	(oom)
DNS	62.9%	2632ms	(oom)	98.4%	972ms	(oom)	97.9%	841.3ms	(oom)

Table 6: Average cache hit rates and isosurface computation performance for the data sets and benchmarks performed. Isosurfaces are typically sparse and occupy neighboring regions of the domain, leading to high cache rates for the sweep benchmarks. The topology of the nested isosurfaces also allows for high hit rates on random isovalues due to the high amount of overlap, whereas the turbulent sheet isosurfaces do not overlap as much and see far lower hit rates. Although the cache space required for the Miranda and DNS is small enough to fit in the Surface Pro's 3.8GB VRAM, for most isovalues, the cumulative size of the cache and output vertex data is not.

Although the sweep up and down benchmarks may seem to be the same, the cache behavior of the two differ on the nested isosurfaces. On these data sets, an up sweep will frequently operate in cache, as the number of active blocks decreases and the inner surfaces are likely to require blocks that were already decompressed for the previous containing surface. However, a down sweep is less likely to hit cache, as the surface area of the isosurface increases to cover more blocks, with these blocks less likely to be cached.

As before, the isovalues are sampled over a value range covering surfaces typically of interest to users, excluding noise and values so high as to produce few output triangles. Example configurations for each data set are shown in Table 5. In each benchmark, we discard the first computation as we have found WebGPU to have a high first launch overhead. The average cache hit rates and extraction time for the benchmarks are shown in Table 6.

On the nested isosurface data sets, we observe high cache hit rates for all three benchmarks, with Sweep Down performing the worst on average due to the lower cache hit rate. A lower cache hit rate means a larger number of blocks must be decompressed to compute each surface, impacting compute time. It is interesting to note that Random achieves a higher hit rate than Sweep Down. After computing some sampling of the nested isosurfaces in Random, the cache contains the most frequently used blocks across these surfaces, allowing for high cache hit rates and better performance.

In contrast, on the turbulent sheet data sets, we observe high cache hit rates on the Sweep benchmarks and low hit rates on Random. When computing random isovalues, the surface can make large jumps in the domain, covering entirely different regions of the volume. This issue is exacerbated by the high resolution of the data sets and the turbulent nature of the computed isosurfaces, leading to a large number of blocks covered by each surface with few shared between them. As a result, large numbers of blocks must be decompressed each time, severely impacting compute time. However, the surface does not move significantly when sweeping the isovalue up or down, resulting in high cache hit rates and better performance.

As indicated by the cache hit rates, we find that on the nested isosurface data sets so few new blocks must be decompressed to compute each new surface (on average, $< 0.5\%$ of the total blocks in the data set) that decompression does not occupy a large portion of compute time. The bulk of time is spent in the first pass to select the active blocks and the mark new items step of the cache update, the latter of which then determines no new items are to be added.

In contrast, on the turbulent sheet data sets a larger percentage of time is spent in decompression due to the higher miss rate and higher absolute number of active blocks. On the random benchmarks, decompression occupies an average of 63% of compute time, with an average of 12% of blocks decompressed for each new surface. On the sweep benchmarks, time is more evenly divided among decompression, finding active blocks, and updating the cache, with an average of 0.8% of blocks decompressed for each new surface.

We find that when new items need to be added to the cache, the bulk of the cache update time is spent sorting the available slots by age. In WebGPU we do not have access to optimized libraries such as Thrust [6] and VTK-m [30], and our sort by key implementation becomes a bottleneck.

4.6.2 Rendering Performance

We report the framerate for the example isosurfaces computed in Table 5 in Table 7. The output of our isosurface computation is a triangle soup in our compressed vertex format, which we render with WebGPU. On both the Surface Pro 7 and RTX 2070, we achieve real-time rendering performance, even for large isosurfaces. Although our rendering modality is relatively simple, these results are encouraging for large-scale data visualization in general, demonstrating that WebGPU can achieve high framerates for large geometry. The quality of the isosurfaces are primarily dependent on the reconstruction accuracy of the compression method, which have demonstrated high accuracy even at high compression ratios [14, 15, 24].

Dataset	Triangles	RTX 2070 (FPS)	Surface Pro 7 (FPS)
Skull	2.1M	180	44
Foot	743K	174	89
Backpack	6.2M	146	25
Plasma	9.5M	118	24
Stag Beetle	6.7M	139	19
Kingsnake	10.2M	128	24
Chameleon	11.2M	123	19
Miranda	67M	53	(oom)
DNS	135M	36	(oom)

Table 7: Rendering performance for the isosurfaces shown in Table 5. We find that WebGPU is capable of interactive rendering of large triangle meshes even on lightweight clients.

We note that, as the vertex buffer occupies a substantial amount of memory, it would be valuable to explore applying implicit isosurface raycasting methods on top of the existing block structure. The blocks can be seen as a macrocell grid [32] for space-skipping, and implicit isosurface ray tracing performed within these blocks.

5 Conclusion: A Roadmap for Client-side Scientific Visualization in the Browser

We have conducted an experimental assessment of the suitability of the browser for building scalable scientific visualization applications, and conclude that by leveraging WebAssembly and WebGPU, it is possible to deliver powerful visualization applications that run entirely in the client's browser. We have shown that native libraries can be compiled to WebAssembly to deploy them in the browser without a significant porting effort or loss of performance. Moreover, we have found that WebGPU's modern low overhead rendering and compute API can achieve performance on par with native Vulkan implementations. With our GPU parallel isosurface extraction algorithm for block-compressed data, we have demonstrated that interactive isosurface computation on massive data sets can be achieved entirely in the browser by making the appropriate algorithm design choices and precision and resolution trade-offs. We hope that this work can serve as a call to action and motivate further efforts to bring scientific visualization to client-side browser applications.

The biggest challenge faced when bringing scientific visualization to the web is the lack of available libraries compiled to WebAssembly or leveraging WebGPU. Having researchers or developers track down the potentially large chain of dependencies required to compile their needed libraries to WebAssembly or implement the complex GPU parallel primitives needed by their algorithm is clearly undesirable. Providing packages with generated bindings for widely used libraries, such as VTK, would be valuable. A package providing optimized WebGPU implementations of data-parallel primitives similar to Thrust [6] and VTK-m [30], would be critical to ease development of applications that process large data sets.

Acknowledgments

The authors wish to thank Duong Hoang for providing compressed versions of the DNS and Stefan Zellmann for valuable discussions. This work was funded in part by NSF OAC awards 1842042, 1941085, NSF CMMI awards 1629660, LLNL LDRD project SI-20-001. This material is based in part upon work supported by the Department of Energy, National Nuclear Security Administration (NNSA), under award DE-NA0002375. This research was supported in part by the Exascale Computing Project (17-SC-20-SC), a collaborative effort of the U.S. Department of Energy Office of Science and the NNSA. This work was performed in part under the auspices of the U.S. Department of Energy by Lawrence Livermore National Laboratory under Contract DE-AC52-07NA27344.

References

[1] LAStools. `https://github.com/LAStools/LAStools/`.

[2] NVIDIA: CUDA Marching Cubes Example. `https://docs.nvidia.com/cuda/cuda-samples/index.html#marching-cubes-isosurfaces`.

[3] VTK.js. `https://github.com/Kitware/vtk-js`.

[4] WebAssembly. `https://webassembly.org/`.

[5] WebGPU. `https://gpuweb.github.io/gpuweb/`.

[6] N. Bell, J. Hoberock, and C. Rodrigues. THRUST: A productivity-oriented library for CUDA. In *Programming Massively Parallel Processors*. 2017.

[7] M. Bostock, V. Ogievetsky, and J. Heer. D^3 Data-Driven Documents. *IEEE Transactions on Visualization and Computer Graphics*, 2011.

[8] P. Cignoni, C. Montani, E. Puppo, and R. Scopigno. Optimal Isosurface Extraction from Irregular Volume Data. In *Proceedings of the 1996 Symposium on Volume Visualization*, 1996.

[9] M. Ciżnicki, M. Kierzynka, K. Kurowski, B. Ludwiczak, K. Napierała, and J. Palczyński. Efficient Isosurface Extraction Using Marching Tetrahedra and Histogram Pyramids on Multiple GPUs. In R. Wyrzykowski, J. Dongarra, K. Karczewski, and J. Waśniewski, eds., *Parallel Processing and Applied Mathematics*, 2012.

[10] S. Dias, K. Bora, and A. Gomes. CUDA-Based Triangulations of Convolution Molecular Surfaces. In *Proceedings of the 19th ACM International Symposium on High Performance Distributed Computing - HPDC '10*, 2010.

[11] C. Dyken, G. Ziegler, C. Theobalt, and H.-P. Seidel. High-speed Marching Cubes using HistoPyramids. *Computer Graphics Forum*, 2008.

[12] T. Dykes, A. Hassan, C. Gheller, D. Croton, and M. Krokos. Interactive 3D Visualization for Theoretical Virtual Observatories. *Monthly Notices of the Royal Astronomical Society*, 2018.

[13] M. Gross, C. Lojewski, M. Bertram, and H. Hagen. Fast Implicit KD-Trees: Accelerated Isosurface Ray Tracing and Maximum Intensity Projection for Large Scalar Fields. In *Proc. Computer Graphics and Imaging*, 2007.

[14] D. Hoang, P. Klacansky, H. Bhatia, P. Bremer, P. Lindstrom, and V. Pascucci. A Study of the Trade-off Between Reducing Precision and Reducing Resolution for Data Analysis and Visualization. *IEEE Transactions on Visualization and Computer Graphics*, 2019.

[15] D. Hoang, B. Summa, P. Klacansky, W. Usher, H. Bhatia, P. Lindstrom, P.-T. Bremer, and V. Pascucci. Efficient and Flexible Hierarchical Data Layouts for a Unified Encoding of Scalar Field Precision and Resolution. *IEEE Transactions on Visualization and Computer Graphics, Proceedings of IEEE VIS 2020 (To Appear)*, 2021.

[16] H. Jacinto, R. Kéchichian, M. Desvignes, R. Prost, and S. Valette. A web interface for 3D visualization and interactive segmentation of medical images. In *Proceedings of the 17th International Conference on 3D Web Technology - Web3D '12*, 2012.

[17] A. Jangda, B. Powers, E. D. Berger, and A. Guha. Not So Fast: Analyzing the Performance of WebAssembly vs. Native Code. In *Proceedings of the USENIX Annual Technical Conference*, 2019.

[18] B. Jeong, P. A. Navrátil, K. P. Gaither, G. Abram, and G. P. Johnson. Configurable Data Prefetching Scheme for Interactive Visualization of Large-Scale Volume Data. In P. C. Wong, D. L. Kao, M. C. Hao, C. Chen, R. Kosara, M. A. Livingston, J. Park, and I. Roberts, eds., *IS&T/SPIE Electronic Imaging*, 2012.

[19] S. Jourdain, U. Ayachit, and B. Geveci. ParaViewWeb: A Web Framework for 3D Visualization and Data Processing. *International Journal of Computer Information Systems and Industrial Management Applications.*, 2011.

[20] M. Lee, N. Malaya, and R. D. Moser. Petascale Direct Numerical Simulation of Turbulent Channel Flow on Up to 786K Cores. In *Proceedings of the International Conference on High Performance Computing, Networking, Storage and Analysis*, SC'13, 2013.

[21] M. Lee and R. Moser. Direct Numerical Simulation of Turbulent Channel Flow up to $Re_\tau \approx 5200$. *Journal of Fluid Mechanics*, 6 2015.

[22] J. K. Li and K.-L. Ma. P4: Portable Parallel Processing Pipelines for Interactive Information Visualization. *IEEE Transactions on Visualization and Computer Graphics*, 2018.

[23] J. K. Li and K.-L. Ma. P5: Portable Progressive Parallel Processing Pipelines for Interactive Data Analysis and Visualization. *IEEE Transactions on Visualization and Computer Graphics*, 2019.

[24] P. Lindstrom. Fixed-Rate Compressed Floating-Point Arrays. *IEEE Transactions on Visualization and Computer Graphics*, 2014.

[25] B. Liu, G. J. Clapworthy, F. Dong, and E. Wu. Parallel Marching Blocks: A Practical Isosurfacing Algorithm for Large Data on Many-Core Architectures. *Computer Graphics Forum*, 2016.

[26] Y. Livnat, H.-W. Shen, and C. R. Johnson. A Near Optimal Isosurface Extraction Algorithm Using the Span Space. *IEEE transactions on Visualization and Computer Graphics*, 1996.

[27] W. E. Lorenson and H. E. Cline. Marching Cubes: A High Resolution 3D Surface Construction Algorithm. *SIGGRAPH Computer Graphics*, 1987.

[28] S. Martin, H.-W. Shen, and P. McCormick. Load-Balanced Isosurfacing on Multi-GPU Clusters. In *Eurographics Symposium on Parallel Graphics and Visualization*, 2010.

[29] M. M. Mobeen and L. Feng. High-Performance Volume Rendering on the Ubiquitous WebGL Platform. In *2012 IEEE 14th International Conference on High Performance Computing and Communication & 2012 IEEE 9th International Conference on Embedded Software and Systems*, 2012.

[30] K. Moreland, C. Sewell, W. Usher, L.-t. Lo, J. Meredith, D. Pugmire, J. Kress, H. Schroots, K.-L. Ma, H. Childs, M. Larsen, C.-M. Chen, R. Maynard, and B. Geveci. VTK-m: Accelerating the Visualization Toolkit for Massively Threaded Architectures. *IEEE Computer Graphics and Applications*, 2016.

[31] F. Mwalongo, M. Krone, G. Reina, and T. Ertl. State-of-the-Art Report in Web-based Visualization. *Computer Graphics Forum*, 2016.

[32] S. Parker, P. Shirley, Y. Livnat, C. Hansen, and P.-P. Sloan. Interactive Ray Tracing for Isosurface Rendering. In *Visualization'98. Proceedings*, 1998.

[33] F. Perez and B. E. Granger. IPython: A System for Interactive Scientific Computing. *Computing in Science & Engineering*, 2007.

[34] M. Raji, A. Hota, T. Hobson, and J. Huang. Scientific Visualization as a Microservice. *IEEE Transactions on Visualization and Computer Graphics*, 2018.

[35] M. Raji, A. Hota, and J. Huang. Scalable Web-Embedded Volume Rendering. In *2017 IEEE 7th Symposium on Large Data Analysis and Visualization (LDAV)*, 2017.

[36] A. Satyanarayan, D. Moritz, K. Wongsuphasawat, and J. Heer. Vega-Lite: A Grammar of Interactive Graphics. *IEEE Transactions on Visualization and Computer Graphics*, 2017.

[37] A. Satyanarayan, K. Wongsuphasawat, and J. Heer. Declarative interaction design for data visualization. In *Proceedings of the 27th Annual ACM Symposium on User Interface Software and Technology - UIST '14*, 2014.

[38] L. Schmitz, L. F. Scheidegger, D. K. Osmari, C. A. Dietrich, and J. L. D. Comba. Efficient and Quality Contouring Algorithms on the GPU. *Computer Graphics Forum*, 2010.

[39] W. Schroeder, K. Martin, and B. Lorenson. *The Visualization Toolkit: An Object-Oriented Approach to 3D Graphics*. 4 ed., 2006.

[40] W. Schroeder, R. Maynard, and B. Geveci. Flying Edges: A High-Performance Scalable Isocontouring Algorithm. In *Large Data Analysis and Visualization (LDAV), 2015 IEEE 5th Symposium On*, 2015.

[41] M. Schütz. Potree: Rendering Large Point Clouds in Web Browsers, 2016.

[42] T. Sherif, N. Kassis, M.-Ã. Rousseau, R. Adalat, and A. C. Evans. BrainBrowser: Distributed, Web-Based Neurological Data Visualization. *Frontiers in Neuroinformatics*, 2015.

[43] C. Stolte, D. Tang, and P. Hanrahan. Polaris: A System for Query, Analysis, and Visualization of Multidimensional Relational Databases. *IEEE Transactions on Visualization and Computer Graphics*, 2002.

[44] I. Wald, H. Friedrich, G. Marmitt, P. Slusallek, and H.-P. Seidel. Faster isosurface ray tracing using implicit KD-trees. *IEEE Transactions on Visualization and Computer Graphics*, 2005.

[45] A. Zakai. Emscripten: An LLVM-to-JavaScript Compiler. In *Proceedings of the ACM International Conference Companion on Object Oriented Programming Systems Languages and Applications Companion - SPLASH '11*, 2011.